Relation Between Critical Current Density and Flux Flow Resistivity in Bi2223 Bulk Element for Fault Current Limiter

T. Aritake, T. Noda, H. Shimizu, Y. Yokomizu, T. Matsumura, and N. Murayama

***Abstract*—The relation between the critical current density and flux flow resistivity in a Bi2223 bulk for fault current limiter was experimentally investigated. The distributions of J_c and voltage along the longitudinal direction were measured as well as transport current. As a result, it is found that the flux flow resistivity is the higher of at the position with lower critical current. Measured results was numerically analyzed to obtain the empirical expression for the flux flow resistivity as a function of the critical current density, accumulated Joule heat and transport current.**

***Index Terms*—Bi2223 bulk, critical current density, fault current limiter, flux flow resistance.**

I. Introduction

As a promising candidate for current limiting technology in electric power system, the introduction of fault current limiter (FCL) is expected [1]. FCL is classified into various types. There is a superconducting FCL as one of them. A typical superconducting FCL is a resistive type which reduces the fault current by the resistance generated by overcurrent flowing in the superconducting element. The FCL may have the problem it requires somewhat time to recover to normal operating state after the fault clearing.

In order to solve the problem of recovery time in the superconducting FCL, we have proposed to use the flux flow resistance of high temperature superconductor (HTS) [2]. Under the state that the temperature of the HTS is below the critical temperature, the flux flow resistance appears in HTS when the transport current exceeds the critical current and disappears at the moment that the current is less than the critical current. It means that the FCL using the flux flow resistance of HTS (a flux flow resistance type of FCL) possibly recovers to normal operating state after the fault clearing, immediately.

In this paper, the generating process of the flux flow resistance is experimentally investigated to obtain fundamental data for the discussion on the feasibility of the flux flow resistance type of FCL using a Bi2223 bulk as the superconducting material [2]. We supplied a sinusoidal overcurrent to the sample of the bulk to measure the distribution of the critical current density and v–j characteristics. Then, the flux flow resistance was expressed as a function of critical current density, accumulated Joule heat and transport current. As a result, it is found that there is a significant correlation between the generated flux flow resistance and the critical current density.

Manuscript received August 5, 2002. This work is supported in part by the Ministry of Education, Culture, Sports, Science and Technology of Japan under Grant-in-Aid for Young Scientists (B)(14750206).

T. Aritake, T. Noda, H. Shimizu, Y. Yokomizu, and T. Matsumura are with the Department of Electrical Engineering, Nagoya University, Furo-cho, Chikusa-ku, Nagoya 464-8603, Japan (e-mail: t_aritak@echo.nuee.nagoya-u.ac.jp).

N. Murayama is with Synergy Materials Research Center, National Institute of Advanced Industrial Science and Technology, Shimo-Shidami, Moriyama-ku, Nagoya 463-8560, Japan.

Digital Object Identifier 10.1109/TASC.2003.812983

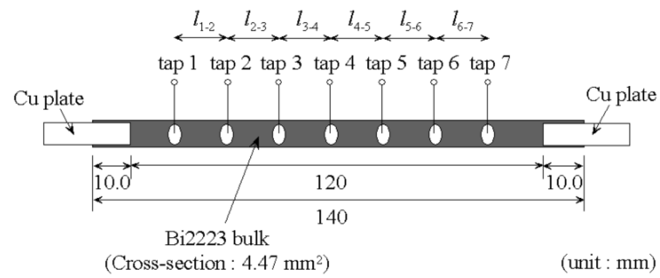

Fig. 1. Sample of Bi2223 bulk adopted.

TABLE I
INTERVALS BETWEEN VOLTAGE TAPS

	l_{1-2}	l_{2-3}	l_{3-4}	l_{4-5}	l_{5-6}	l_{6-7}
Sample 1 (mm)	15.3	14.2	15.1	15.1	14.8	14.2
Sample 2 (mm)	14.6	13.5	15.8	14.5	15.6	15.9

II. Bi2223 Bulk Sample

We adopted a Bi2223 bulk made by sintering [3] as the sample conductor. We took the measurement for two samples (sample 1 and sample 2). Fig. 1 illustrates the shape of the samples. The length l and cross-sectional area S of both samples are 140 mm and 4.47 mm^2, respectively. As shown in Fig. 1, copper plates were soldered at both ends of the sample as the electrodes. The voltage taps 1 to 7 were connected along the longitudinal direction to measure the distributions of the critical current density and flux flow resistivity. The intervals between taps are listed in Table I.

Fig. 2 shows the critical current density J_{c0} measured under the conditions of 77 K and 0 T at each section in the samples. The somewhat dispersion of J_{c0} exists. The averages of J_{c0} in sample 1 and sample 2 are 2.48×10^7 A/m^2 and 1.62×10^7 A/m^2, respectively. The ranges of the dispersion of J_{c0} for sample 1 and sample 2 are 0.46×10^7 A/m^2 and 0.80×10^7 A/m^2, respectively.

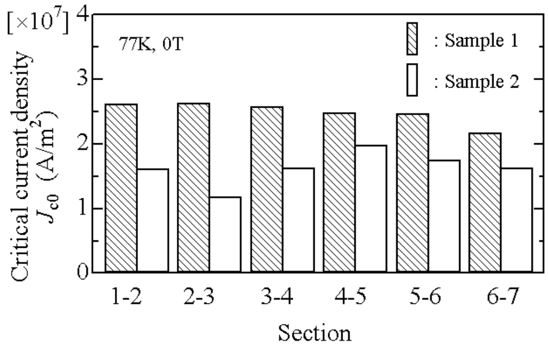

Fig. 2. Distribution of critical current density.

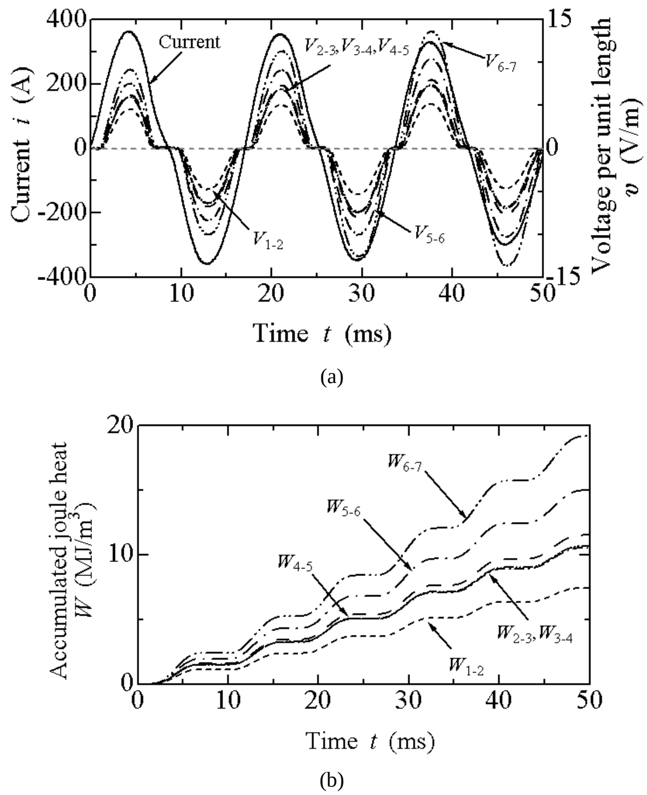

Fig. 3. Waveforms of current, voltage per unit length and accumulated Joule heat (sample 1). (a) Current and voltage per unit length. (b) Accumulated Joule heat.

III. Overcurrent Carrying Test

A.C. (60 Hz) overcurrent was suddenly supplied to the sample for three cycles. For the various peak values of the overcurrent, the transport current and voltage across each section were measured and then the accumulated Joule heat generated in each section was estimated.

Fig. 3 shows the example of measured waveforms of the current i, voltage v generated per unit length and accumulated Joule heat W per unit volume at each section in sample 1. The maximum values of current is 365 $\mathrm{A_{peak}}$ in this example. We obtained W by integrating the product of instantaneous value of current density j ($=i/S$) and v.

When i exceeds the critical current level of the section, v appears because the sample begins to exhibit the flux flow resistance. The voltage v disappears at the moment that i becomes lower level than critical current. The accumulated Joule heat W increases as the time proceeds. The temperature of the bulk must rise with W. Since the flux flow resistance increases by the temperature rise, the peak value of v grows with the elapse of time. As shown in Fig. 3(a), the magnitude of v depends on the section in the sample. From Fig. 2 and Fig. 3(a), it is found that large voltage trends to be generated in the section which has low J_{c0}. This tendency is also observed in sample 2.

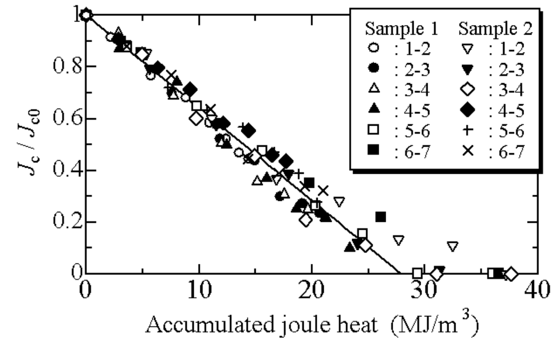

Fig. 4. Critical current density as a function of accumulated Joule heat.

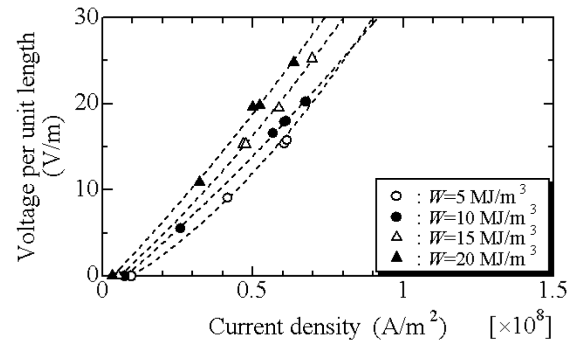

Fig. 5. Voltage-current density characteristics at Sections II and III in sample 2 ($J_{c0} = 1.10 \times 10^{7}$ A/m²).

IV. Relation Between Critical Current Density and Joule Heat

We can obtain the critical current density J_c by reading the current level at the moment when v becomes zero in Fig. 3(a). In Fig. 4, the measured values of J_c are plotted against the accumulated Joule heat W at that time, which can be gotten from Fig. 3(b). The value of J_c of a vertical axis in Fig. 4 is normalized by J_{c0}. From Fig. 4, J_c linearly decreases with an increase in W at every section. It is found that the results for all sections do not differ much. By the method of least squares, we obtained the equation of the relation between J_c/J_{c0} and W (unit: MJ/m³) approximated as the linear function as follows:

$$\frac{J_c(W)}{J_{c0}} = -3.58 \times 10^{-8} W + 1. \tag{1}$$

V. Voltage-Current Density Characteristics

The relation between the voltage v per unit length and the current density j (v–j characteristics) may also depend on W. We can also derive the dependence of v–j characteristics on W

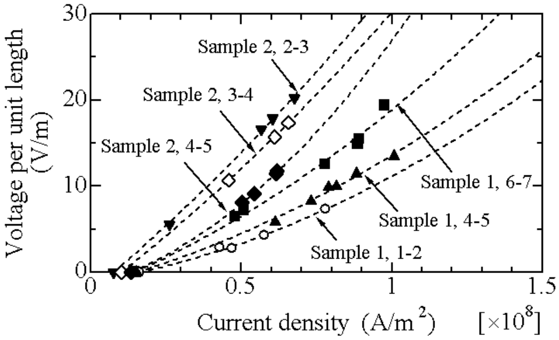

Fig. 6. Voltage-current density characteristics ($W = 10$ MJ/m^3).

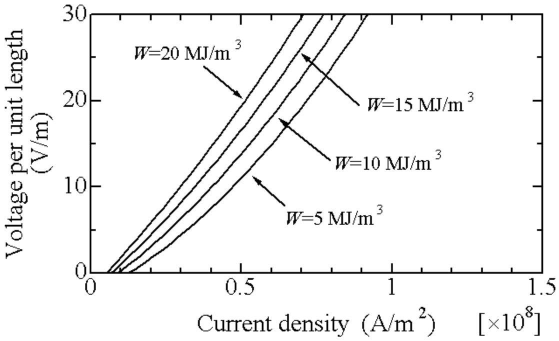

Fig. 7. Voltage-current density characteristics at Sections II and III in sample 2 estimated from (2)∼(9) ($J_{c0} = 1.10 \times 10^7$ A/m^2).

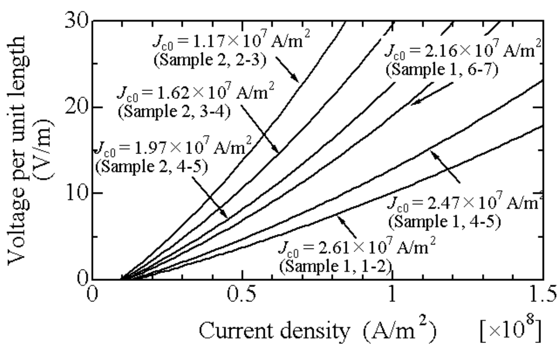

Fig. 8. Voltage-current density characteristics estimated from (2)∼(9) ($W = 10$ MJ/m^3).

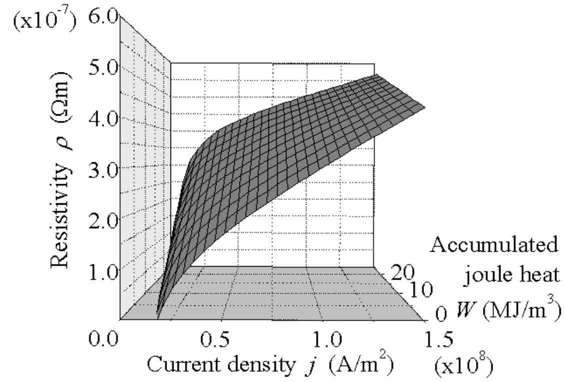

(a)

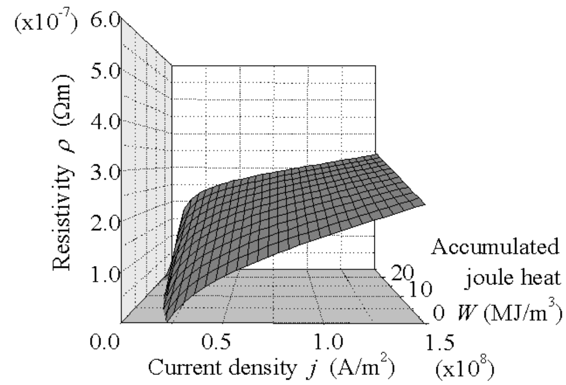

(b)

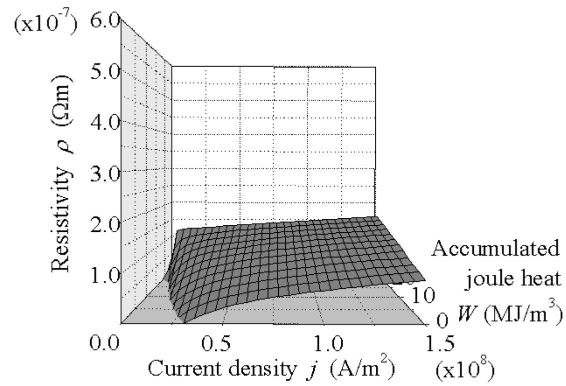

(c)

Fig. 9. Resistivity-current density characteristics. (a) $J_c = 1.17 \times 10^7$ A/m^2 (b) $J_c = 1.97 \times 10^7$ A/m^2 (c) $J_c = 2.61 \times 10^7$ A/m^2.

from Fig. 3(a) and (b) [2]. Fig. 5 shows the example of results obtained for the Sections II and III in sample 2 with some kinds of dots. This figure indicates the v–j characteristics for $W = 5$, 10, 15, and 20 MJ/m^3. The dots on a transverse axis are equivalent to J_c for each W, and determined by (1). The broken lines in Fig. 5 correspond to the curves approximated as quadratic expression by the method of least squares. From Fig. 5, v increases with W as well as j. We have confirmed that the other sections and another sample also have the same tendency.

The v–j characteristics under $W = 10$ MJ/m^3 obtained for some sections are indicated together in Fig. 6. The broken lines are the approximated ones. From Figs. 2 and 6, the magnitude of v and slope of v–j characteristics in the section which has lower J_{c0} are larger than that in the section with higher J_{c0}. This tendency is also found for other W.

VI. Numerical Formulation of v–j Characteristics

We assumed that v was expressed as a quadratic function of j as next equation

$$v(j,\, J_{c0},\, W) = a_0(J_{c0},\, W) + a_1(J_{c0},\, W)j + a_2(J_{c0},\, W)j^2 \tag{2}$$

where a_0, a_1 and a_2 are supposed to be presented as functions of J_{c0} and W. We obtain the value of a_0, a_1, and a_2 for different W and sections by approximating v–j characteristics to quadratic expression with method of least squares. It is assumed that a_0, a_1, and a_2 are written as linear function of J_{c0} as follows:

$$a_i(J_{c0},\, W) = b_{i0}(W) + b_{i1}(W)J_{c0} \qquad (i = 0,\, 1,\, 2) \tag{3}$$

where b_{i0} and b_{i1} are supposed to be expressed with a function of only W. By the method of least squares, the relation between $J_{\rm c0}$ and all a_i was approximated with linear function and then we obtained the coefficients b_{i0} and b_{i1}. Furthermore, we assumed that b_{i0} and b_{i1} could be expressed by a linear function of W. Then, we can obtain the dependence of all b_{i0} and b_{i1} on W as follows:

$$b_{00}(W) = -3.19 + 7.19 \times 10^{-5} W \tag{4}$$

$$b_{01}(W) = 4.26 \times 10^{-8} + 3.33 \times 10^{-9} W \tag{5}$$

$$b_{10}(W) = 1.51 \times 10^{-7} + 2.08 \times 10^{-8} W \tag{6}$$

$$b_{11}(W) = -3.54 \times 10^{-15} - 6.89 \times 10^{-16} W \tag{7}$$

$$b_{20}(W) = 3.76 \times 10^{-15} - 8.33 \times 10^{-17} W \tag{8}$$

$$b_{21}(W) = -1.33 \times 10^{-22} + 3.15 \times 10^{-24} W. \tag{9}$$

As a result, (2)–(9) enable us to quantitively estimate the v–j characteristics of our Bi2223 bulk for any W and $J_{\rm c0}$. In Fig. 7, the v–j characteristics for $J_{\rm c0} = 1.10 \times 10^{-7}$ A/m^2 are illustrated for some kinds of W, whose calculation conditions correspond to the experimental ones of Fig. 5. Fig. 8 shows the v–j characteristics for $W = 10$ MJ/m^3 for different $J_{\rm c0}$s. This figure corresponds to Fig. 6 because $J_{\rm c0}$ was measured for each section as shown in Fig. 2. It is confirmed that the calculated curves almost agree with the measured results by the comparison between Figs. 7 and 5 and between Figs. 8 and 6.

VII. Resistivity-Current Density Characteristics

General expressions on the flux flow resistance must be useful for computing the current limiting performance of the flux flow resistive type of FCL. The resistivity ρ is obtained by division of v by corresponding j as follows:

$$\rho(j,\, J_{\rm c0},\, W) = \frac{a_0(J_{\rm c0},\, W)}{j} + a_1(J_{\rm c0},\, W) + a_2(J_{\rm c0},\, W)j. \tag{10}$$

Fig. 9 represents ρ calculated from (3)–(10) as functions of j and W in cases of $J_{\rm c0} = 1.17 \times 10^7$, 1.97×10^7 and 2.61×10^7 A/m^2 as an example. It is found that ρ changes with j, W and $J_{\rm c0}$. As far as our Bi2223 bulk made by sintering is concerned, the lower $J_{\rm c0}$ bulk has the higher resistivity in the flux flow resistance state as seen from Fig. 9.

VIII. Conclusion

We investigated the dependence of the flux flow resistance on the instantaneous value of the transport current, the generated Joule heat and critical current density for the Bi2223 bulk made by sintering. As a result, we were able to express the relation between the normalized critical current density and Joule heat. Furthermore, we were also able to formulate the value of the flux flow resistance using the current density, the Joule heat and the critical current density. As far as our Bi2223 bulk is concerned, the magnitude of the flux flow resistivity for the section which has the lower critical current density are larger than that for the section with the higher critical current density. The numerical expression on the flux flow resistivity, which were formulated from the experimental v–j characteristics, will enable us to evaluate the current limiting performance of the flux flow type FCL with Bi2223 bulk.

References

[1] E. Leung, “Surge protection for power grids,” *IEEE Spectrum*, pp. 26–30, July 1997.

[2] H. Shimizu, Y. Yokomizu, T. Matsumura, and N. Murayama, “Proposal of flux flow resistance type fault current limiter using high Tc superconducting bulk,” IEEE Trans. Appl. Superconduct., to be published.

[3] N. Murayama and J. B. Vender, “Densification behavior during hot pressing of Bi-Pb-Sr-Ca-Cu-O superconductors,” *Physica C*, vol. 256, pp. 156–160, 1996.